J Ther Eng, Vol. 11, No. 1, pp. 226−239, January, 2025

Journal of Thermal Engineering
Web page info: https://jten.yildiz.edu.tr
DOI: 10.14744/thermal.0000915

Research Article

Thermal conductivity of porous plastics manufactured by 3D printing: Controlling the design of the cavities and corresponding effects

Ahmed K. MUHAMMAD[1], Tawfeeq W. MOHAMMED[1,*], Kadhim K. RESAN[1]

[1]*Department of Materials, Mustansiriyah University, College of Engineering, 10052, Iraq*

ARTICLE INFO

Article history
Received: 05 December 2023
Revised: 26 February 2024
Accepted: 26 February 2024

Keywords:
3D Printing; Additive Manufacturing; Cavities; Insulation; Thermal Conductivity

ABSTRACT

This study examines factors associated with the cavities formed in 3D-printed porous thermoplastics, and establishes their relationship with the thermal conductivity of bulk material. The research has examined two porous thermoplastics, specifically poly-lactic acid (PLA) and acrylonitrile butadiene styrene (ABS). Certain categories have been used for the cavities based on their shapes (sphere, cube and diamond), sizes (0.5 to 1.9 mm), numbers (200 to 500), and distributions (in-line or staggered). Specific findings indicate that the optimal thermal conductivity value can be achieved by utilizing samples with 500 pores of 1.5 mm pore diameter. It is shown, the pores could be in the shape of diamonds and distributed in a staggered manner in order to have minimum thermal conductivity. The thermal conductivity values for the most favorable specimens were determined to be 0.13 W/m·K for PLA and 0.12 W/m·K for ABS. The observed values demonstrate a decrease of 40-45% in comparison to the non-porous samples of the same materials.

Cite this article as: Muhammad AK, Mohammed TW, Resan KK. Thermal conductivity of porous plastics manufactured by 3D printing: Controlling the design of the cavities and corresponding effects. J Ther Eng 2025;11(1):226−239.

INTRODUCTION

Polymers can be classified into two categories: naturally occurring polymers and synthesized polymers. Cellulose and natural rubber are well known as natural polymers. Conversely, a considerable array of synthetic polymers, which are artificially produced, can be observed in diverse manifestations such as fibers, elastomers, plastics, adhesives, and other forms. Every family inherently consists of numerous subgroups. Polymers can be categorized based on their structure or behavior, as outlined in references [1] and [2].

1. Natural or synthetic
2. Homo-polymer or copolymer
3. Linear, branched or cross-linked.
4. Amorphous or crystalline
5. Thermoplastics or thermosets

A thermoplastic is a polymer which exhibits the property of being flexible or capable of being shaped when exposed to a specific higher temperature, and then reverts to a solid state when subjected to lower temperatures. This kind of materials undergoes a phase transition in which it melts upon heating and subsequently solidifies upon cooling.

*Corresponding author.
*E-mail address: tawfeeqwasmi@uomustansiriyah.edu.iq

This paper was recommended for publication in revised form by Editor-in-Chief Ahmet Selim Dalkılıç

Published by Yıldız Technical University Press, İstanbul, Turkey

This implies that they possess the potential for reuse and can undergo the process of recycling. Thermoplastics encompass a diverse array of polymers that often exhibit a common set of characteristics and capabilities. The primary categories of thermoplastics consist of polymers derived from polyethylene or polystyrene. Thermoplastics can be categorized based on their structural characteristics as either crystalline or amorphous, or based on the composition of their components as either homo-polymer or co-polymer. Moreover, these entities can be categorized based on their molecular structures, namely into two distinct types: linear and branched. Thermoplastics are utilized in the production of a diverse array of objects, including tools, frames, channels, panels, containers, bags, and buckets [3, 4].

The thermal conductivity of a substance is a quantitative representation of its capacity to conduct thermal energy. This statement elucidates the mechanism through which thermal energy is conducted within the solid component. The aforementioned characteristic is widely recognized in academic literature as the k-value of the material. A material with a low k-value is indicative of its favorable thermal insulating properties. The thermal conductivity of a material is influenced by various parameters, including temperature, density, porosity, wetness, degree of crystallinity, chain structure, grain orientation, molecular size, and presence of impurities [5, 6].

Porosity is a crucial property that has a significant impact on the thermal conductivity value of porous materials. The morphology of a material and its accompanying thermal properties are directly influenced by the quantity, size, and form of its pores [7, 8]. The presence of significant porosity within the material is a method employed to obtain an adequate thermal insulation material [9]. The inclusion of pores in the polymeric material leads to a reduction in bulk density, resulting in fewer thermal bridges. Additionally, the presence of pores contributes to the repulsion of heat flow due to the lower thermal conductivity of air (or gas) in the vacancies compared to the core solid materials [10]. Hence, a decline in the overall thermal conductivity of the bulk material has been observed [11, 12]. The inclusion of nano-scale pores in a porous material leads to a further drop in its effective thermal conductivity. This phenomenon can be attributed to the significant diffuse scattering of heat that occurs within the nano-cells [13]. Nano-porous materials have pore diameters that are in close proximity to the mean free path of the fill gas, resulting in a reduction in molecular collisions [14]. The Knudsen effect is observed in nano-materials, where it leads to a significant decrease in the thermal conductivity of the bulk core. This drop occurs when the size of the cavity is less than the mean free path of the air (or gas) present within the material. In this particular scenario, it can be observed that the gas particles will come into contact with the surfaces of the cavities, but they lack the capacity to effectively transfer heat [15, 16]. Conversely, previous studies have indicated that the composition of the gas within the pore significantly influences the thermal insulation capabilities of the material [17-19]. Nevertheless, the primary characteristics that contribute to super-insulation include low density, high porosity, tiny cell size, and solid interruptions that impede the transfer of phonons [20].

The utilization of 3D printing, which is a form of additive manufacturing, has emerged as a sophisticated technique for fabricating three-dimensional items through the translation of digital 3D models into physical structures. The task can be accomplished by two methods: material deposition or the process of melting and subsequent solidification, both of which are executed under computer control. The addition of filling materials, such as polymers or powders, can be facilitated by a designated port [21]. The filaments utilized in the casting procedure may exhibit variations in their geometries, although they are typically obtainable as circular-shaped rolls of plastic wires with specific diameters ranging from 1.75 to 3 mm [22]. The majority of utilized plastic filaments include PLA, ABS, PA and PET [23, 24]. Usually, the plastics in use consist of virgin ingredients, but in limited cases a certain amount of recycled plastics may be involved [25]. Thermoset polymers can also be utilized in conjunction with appropriate curing techniques [26]. The utilization of polymer-based composites presents a viable option in specific applications, as it offers the potential to boost mechanical strength [27, 28] and improve heat conductivity [29]. According to existing literature, the prevailing techniques employed in the field of 3D printing are as follows [30]:

1. Fused deposition modeling (FDM) is one of the most prevalent forms of 3D printing. In this manufacturing process, a nozzle extrudes molten plastic material in layers to compose the sample.
2. Stereolithography (SLA) is a common technique in which a laser-assisted mechanism is utilized, usually for the printing of thermosetting polymers. The laser is responsible for the process of curing the material after casting, known as "photo-polymerization".
3. Selective laser sintering (SLS) is a manufacturing process that utilizes a laser beam to induce the fusion of plastic material, which is initially in a powdered form. This technique has the capability to produce highly accurate products in suitable costs.

Lately, it has been a growing interest in the utilization of 3D printing technology for the production of polymeric components with diverse features. This interest stems from the wide range of applications, such as: construction, electrical and many thermal purposes especially those related to thermal insulation. Table 1 shows the available studies that related to the current study as a literature, or involved in understanding design parameters under study. The selection is based upon the contribution of these studies in elaborating the value of thermal conductivity (k-value). Most of these studies have involved 3D-printing in developing the material for the thermal insulation purpose. Note

Table 1. Contribution of previous studies within parameter affecting thermal conductivity

Ref.	Materials	Application	Effective parameters	Range of k-value (W/m·K)
[31]	PLA & ABS	Cryogenic temperatures	Printing resolution and layer thickness	0.05-0.2
[32]	Thermoset (DCPD)	Thermal insulation	Ink viscosity and curing temperature	0.08-0.12
[33]	Resin + NPs	Thermal conduction	Content ratio of fillers	0.6-0.7
[34]	Thermoplastic composites	Thermal insulation	Blending ratio and printing temperature	N/A
[35]	PA-12	Hollowed window frame	Number of cavities (100-1000), diameter of cavity (4-10 mm) and shape of cavity (quadratic, hexagonal, and triangle	0.06-0.11
[36]	Composite Nylon/CFRP	Heat exchanger	Content ratio of fibers and distribution	1-4
[37]	Silica-aerogel ink	Thermal insulation	Content ratio of porous aerogel and distribution	0.03-0.05
[38]	Thin solid PLA	Thermal insulation	The thickness of the sample and exposure time to temperature	N/A
[39]	General materials	Many applications	Material's anisotropy	General
[40]	Composite PLA/CB particles	Conductive polymers for sensors	Filament orientation and sample temperature	N/A
[41]	PLA reinforced by copper wire	Heat exchanger	Wire volume fraction and sample thickness	0.22-9.4
[42]	PLA	Thermal insulation	Sample thickness, cooling time and filler content	0.06-0.22
[43]	PC	Thermal insulation	In-fill ratio and printing temperature	0.06-0.18
[44]	Concrete	Insulated walls	Configuration of enclosures and filling material	Less than 0.7
[45]	Polymeric nano-composites	Conductive polymers	Content ratio of fillers	Up to 5
[46]	Nano-porous polymers	Thermal insulation	Porosity and mean temperature	Down to 0.02
[47]	PLA/CF composites	Conductive polymers	Content ratio of fillers	Up to 37
[48]	Cellulose/ aerogel composite	Thermal insulation	Content ratio of aerogel	0.03-0.05
[49]	General polymers	Fire retardant	Content ratio of additives	N/A
[50]	PLA	Thermal and acoustic insulation	Porosity, density and sample thickness	0.037-0.2

that parameters of cavities have been focused on, in case of porous materials. However, the references have been arranged in order of chronological precedence [31-50].

However, the previous studies are mostly focused upon the developing of the thermal conductivity using different materials and techniques, but with a limited concentration upon the role of cavities in controlling the desired k-value. Therefore, the present study aims to link the behavior of thermal conductivity with the configuration of cavities in porous thermoplastics produced through 3D printing, for the purpose of thermal insulation. The originality of this study is to examine the impact of cavities' parameters (quantity of cavities, size of each cavity, configuration of the cavity, and the arrangement of the cavities) on the effective thermal conductivity for 3D-printed porous plastics. The current study presents experimental data and guide for optimal design parameters for such kind of materials.

MATERIALS AND METHODS

The present study necessitates the production of certain samples utilizing 3D printing technology, employing various configurations. Subsequently, the thermal conductivity values (k-values) of these samples are to be measured. The experimental investigations were carried out from January to April of 2023. The samples were developed and fabricated within the Laboratory of Polymers, whereas the k-value tests were conducted within the Laboratory of Testing.

Materials

This study focuses on the utilization of two commonly used filament materials, namely PLA and ABS, manufactured by Zhuhai Sunlu Industrial Co. Ltd. in China. The materials are being delivered in the form of bundles of plastic filaments. The materials in question are classified as virgin thermo-plastic homo-polymers. The thermal characteristics of the aforementioned materials are presented in Table 2.

Design

The initial stage in the production of the specimens involves the design of the sample shapes according to the specified configuration, utilizing appropriate software. The 3D models have been meticulously crafted utilizing SOLIDWORKS Premium 2020 in order to get accurate structures for the specimens, including the cavities. The

Table 2. Thermal properties of selected thermoplastic materials*

Material	Manufacturer	Melting point (°C)	Density (g/cm³)	Filament diameter (mm)
PLA (Gray)	Zhuhai Sunlu Industrial Co. Ltd	190	1.25	1.75
ABS (Black)	Zhuhai Sunlu Industrial Co. Ltd	240	1.05	1.75

*Provided by the data sheet

design can afterwards be converted and utilized by a 3D printer for the production of the necessary samples.

Configurations

The samples exhibit variations in the morphologies and distribution of cavities within their solid core. Several characteristics have been investigated in relation to these cavities, including their shape, size, quantity, distribution, as well as the overall porosity and bulk density. Table 3 enumerates the characteristics of the cavities. In the present investigation, three distinct cavity forms have been chosen, specifically: spherical, cubical, and diamond. A selection of pore sizes ranging from 0.5-1.9 mm has been chosen for the spherical form. This range has been chosen to ensure better distribution of the pores through the entire sample, and to satisfy the limit of the 3D-Printer for any miss-filling, intersection or overlapping. Each sample in the study consists of four layers of cavities arranged across its thickness. The distribution of cavities categorized as either in-line or staggered. In the inline mode, the distribution of the four layers is same. In the staggered mode, there is a shift applied to the inner layers (2 and 4) to evenly distribute the pores across areas that were not previously covered by the preceding layers (1 and 3). The size of a cavity is determined by its diameter in the case of a spherical cavity. However, for cavities with cubical or diamond geometries, the size reflects a dimension that ensures an equivalent volume to that of a sphere. It should be noted that the sample exhibits a total of 204, 348, or 500 cavities, each possessing specific internal distances, as depicted in Figure 1. Two distinct samples will be produced, one for PLA and another for ABS, with the intention of achieving the optimal k-value. This will be determined by analyzing the optimal outcomes obtained from varying the thermal conductivity with respect to factors such as pore diameter, distribution type, number of pores, and pore shape. Therefore, the overall number of samples will amount to 24, as indicated in Table 4, which provides detailed information for each individual sample.

Table 3. Features of the cavities

Feature	Value
Shape of cavity	sphere, cube, diamond
Distribution of cavities	in-line, staggered
Size of cavity (mm)	0.5, 1.0, 1.5, 1.8, 1.9
No. of cavities	204, 348, 500

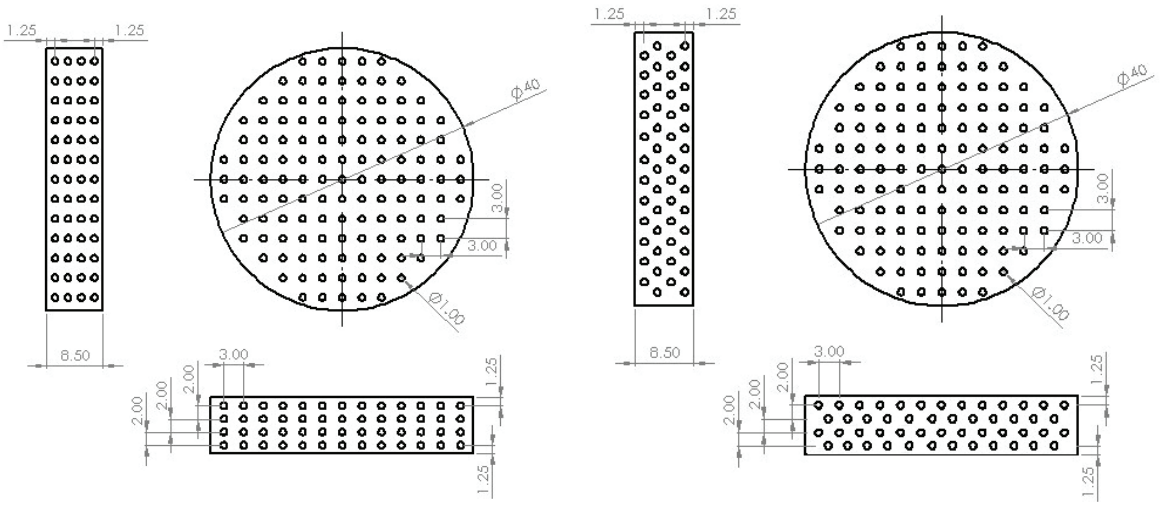

In-line Staggered

Figure 1. Different views of the sample with precise dimensions (500 spherical pores of 1 mm diameter).

Table 4. Details of samples

Type of sample	Details	No. of samples
Spherical	PLA solid sample without cavities as a reference one	1
	PLA porous sample with 0.5 mm diameter, 500 cavities and in-line	1
	PLA porous sample with 1.0 mm diameter, 500 cavities and in-line	1
	PLA porous sample with 1.5 mm diameter, 500 cavities and in-line	1
	PLA porous sample with 1.8 mm diameter, 500 cavities and in-line	1
	PLA porous sample with 1.9 mm diameter, 500 cavities and in-line	1
	PLA porous sample with 1.0 mm diameter, 500 cavities and staggered	1
	PLA porous sample with 1.0 mm diameter, 348 cavities and in-line	1
	PLA porous sample with 1.0 mm diameter, 204 cavities and in-line	1
	ABS solid sample without cavities as a reference one	1
	ABS porous sample with 0.5 mm diameter, 500 cavities and in-line	1
	ABS porous sample with 1.0 mm diameter, 500 cavities and in-line	1
	ABS porous sample with 1.5 mm diameter, 500 cavities and in-line	1
	ABS porous sample with 1.8 mm diameter, 500 cavities and in-line	1
	ABS porous sample with 1.9 mm diameter, 500 cavities and in-line	1
	ABS porous sample with 1.0 mm diameter, 500 cavities and staggered	1
	ABS porous sample with 1.0 mm diameter, 348 cavities and in-line	1
	ABS porous sample with 1.0 mm diameter, 204 cavities and in-line	1
Cubic	PLA porous sample with 1.0 mm equivalent size, 500 cavities and in-line	1
	ABS porous sample with 1.0 mm equivalent size, 500 cavities and in-line	1
Diamond	PLA porous sample with 1.0 mm equivalent size, 500 cavities and in-line	1
	ABS porous sample with 1.0 mm equivalent size, 500 cavities and in-line	1
Optimum	PLA porous sample with 1.5 mm equivalent size (diamond), 500 cavities and staggered	1
Optimum	ABS porous sample with 1.5 mm equivalent size (diamond), 500 cavities and staggered	1
Total		24

Manufacturing

The specimens were manufactured using the Anet ET4 3D printer, which utilizes Fused Deposition Modeling (FDM) printing technique. Table 5 presents an overview of the primary characteristics of the printer. The printing machine has been equipped with the necessary design models and operated to produce samples in batches under appropriate conditions. Figure 2 depicts a series of samples during the printing process.

Table 5. Features of 3D printers*

Feature	Value
Type	Anet ET4
Nozzle diameter (mm)	0.1
Operating temperature (°C)	100-300
Layer thickness (mm)	0.2
Printing speed (mm/s)	50

*Provided by the data sheet

Measuring the Thermal Conductivity Value

The thermal conductivity values were determined using the MED-103 thermal conductivity equipment (Fig. 3), following the guidelines provided in the ASTM C177 standard. The specimens used for testing had a diameter of 40 mm and a thickness of 8.5 mm. The apparatus is comprised of a chamber, heater, heated disc, cold disc, and thermometer. The heater is an electrical apparatus that operates with regulated voltage and current. A pair of K-type wires is affixed to the hot and cold sides respectively, for the purpose of measuring temperature differentials. The specimens ought to be placed into the space that exists between the discs. The measurements supposed to record the steady-state readings for the temperatures. Where, they have been inserted into the one-dimensional heat equation (Fourier equation) to calculate the thermal conductivity, which has been validated for use with the current device. It should be noted that the experiments were conducted multiple times in order to achieve accurate and precise measurements. In order to ensure accurate measurement, the gadget underwent calibration by the Central Organization

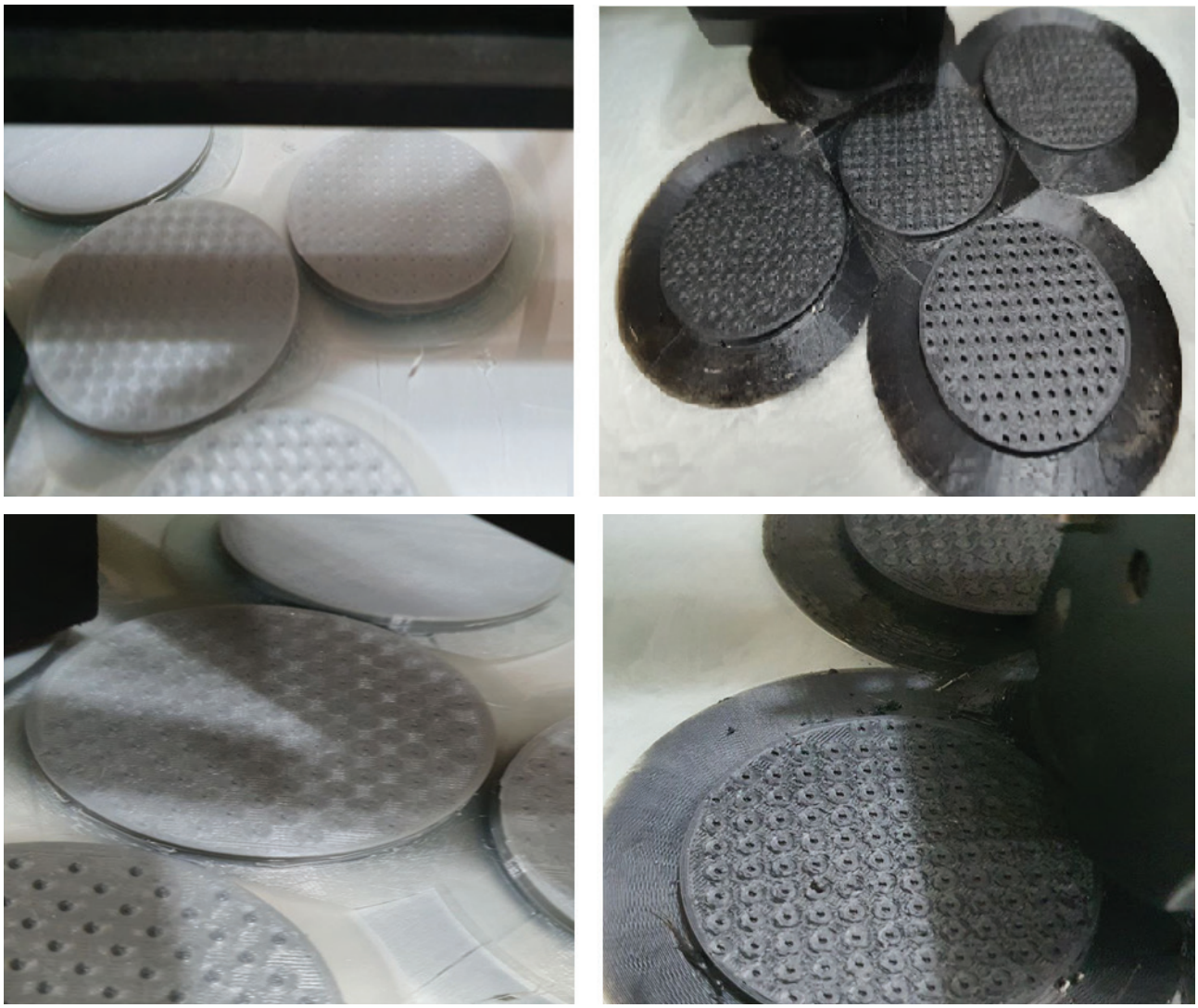

Figure 2. Samples under printing (PLA in gray, and ABS in black).

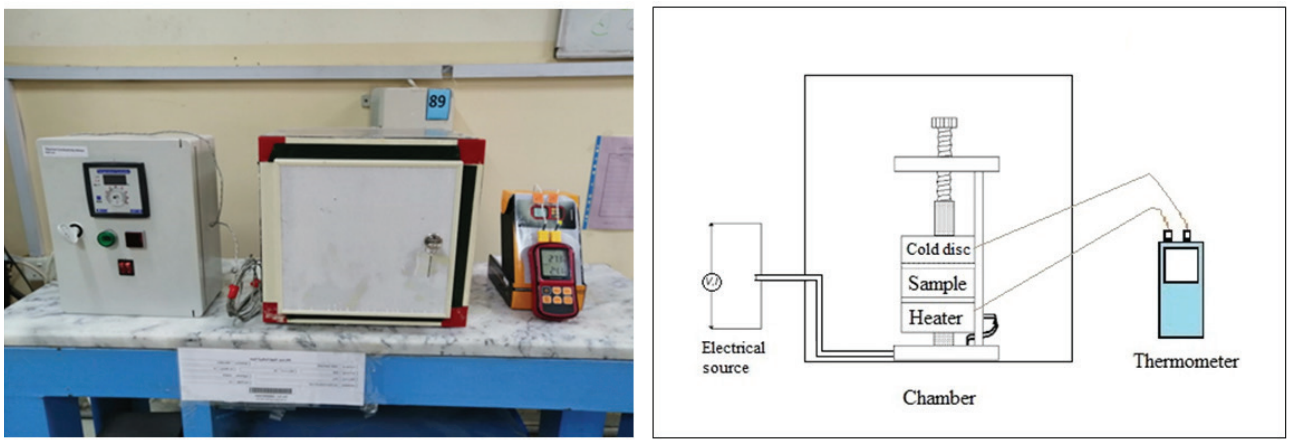

Figure 3. Thermal conductivity apparatus (actual view to the left, and a scheme to the right).

for Standardization and Quality Control (COSQC), resulting in a variance of ±8%.

RESULTS AND DISCUSSION

The study analyzes the thermal conductivity behavior of porous thermoplastics for thermal insulation purposes. The aim is to examine the following effects: number of pores, size and shapes of pores and the distribution of pores. This study provides experimental data, and provides guidance for optimizing the design of porous plastics produced by 3D printing process.

Note that the study supposed no magnetohydrodynamic (MHD) effects since there is no flow, where the application is not assigned for nano-fluids or conductive polymers [51-53].

General Results

The obtained data presents the thermal conductivity values (k-values) for porous plastic panels that were fabricated using 3D printing technology. Table 6 displays the operational circumstances.

In order to understand the impact of cavities on thermal conductivity values, it is advisable to initially examine the individual influence of each parameter on the k-value. Subsequently, the collective effects can be analyzed to assess the combined impact of all parameters, and determine the minimum k-value in overall. Then, a desired sample can be composed to achieve the optimal configuration.

In porous media, heat transport occurs primarily through the interactions of phonons and electrons within the solid or gas components, as well as through convection and radiation modes [54]. The consideration of the convection term is typically omitted in the analysis of small pores due to the limited efficacy of the material's apertures in facilitating air movement under a pressure gradient [55]. According to a publication, the significance of photonic radiation in the overall thermal conductivity of porous media is observed mostly at elevated temperatures [56].

The initial set of findings shows the behavior of the k-value in relation to the quantity of pores, as shown in Figure 4. Generally, any increase in the quantity of pores results in a decrease in the thermal conductivity due to the increased air content ratio. Consequently, this results to a higher thermal resistance [54].

Moreover, it has been observed that the augmentation of pore density exhibits a significant impact on the reduction of phonon transport and its associated mean free path [57]. Hence, the sample containing 500 holes exhibits a lower k-value, ranging from 15% to 25% less, in comparison to the sample with 204 pores.

Additionally, the subsequent set of findings pertains to the fluctuation of the k-value in relation to the pore diameter, as illustrated in Figure 5. Overall, the findings indicate that the k-value exhibits a decreasing trend as the pore size increases, reaching an optimal diameter. Beyond this diameter, the value of k exhibits an upward trend once more. The observed decline in the k-value can be attributed to the concurrent increase in air volume inside the matrix, resulting in larger porosity [57-59]. This is due to the fact that air possesses lower heat conductivity compared to polymeric materials. The optimal results for the k-value of PLA and ABS materials were observed at a thickness of 1.5 mm, with values of 0.17 and 0.14 W/m·K, respectively. Subsequently, the k-value has exhibited a marginal rise as a result of the heightened involvement of the gas component in the overall thermal conductivity within the pore, hence facilitating a greater occurrence of gas-gas interactions in comparison to gas-crystal interactions [60]. Conversely, there is a growing prevalence of radiation heat transfer in the context of big holes [61, 62] or high porosity [63]. Additionally, it has been observed that the impact of phonon scattering on the reduction of the k-value diminishes as the width of the pores increases [58, 64]. Furthermore, it is worth noting that natural convection plays a significant role within this particular range of pore size. However, it is important to highlight that its contribution does not surpass 5% of the effective thermal conductivity value, as mentioned in reference [65].

From the standpoint of the porosity impact, it can be observed that an increase in pore size corresponds to an increase in porosity, resulting in an overall decrease in thermal conductivity [66-68]. Where, the porosity (ϕ) is the ratio between the volume of air to the overall volume occupied by the bulk material. This can be expressed in terms of densities as:

$$\varphi = \left(1 - \frac{\rho_{bulk}}{\rho_{solid}}\right) \text{x } 100\% \quad (1)$$

The density of the aerated sample can be calculated by displacing the amount of air cavities from the original solid mass. Mass of air can be determined by calculating the volume of one pore multiplied by number of cavities, and then multiplying by the air density.

The present investigation revealed a notable rise in porosity, as evidenced by the data presented in Table 7. Specifically, the porosity rose from 1% for the sample with a pore size of 0.5 mm to 18% for the sample with a pore size of 1.9 mm.

Table 6. Operational conditions

Item	Value or description
Materials	PLA & ABS
Dimensions of panels	Disc (40 mm diameter & 8.5 mm thickness)
No. of pores	204-500
Pore diameter	0.5-1.9 mm
shapes of pores	Sphere, cube and diamond
Distribution of pores	In-line & staggered
Gas in pores	Air at standard ambient conditions

Table 7. Effect of porosity on the thermal conductivity value

Pore size (mm)	Porosity of the sample (%)
0.0	0
0.5	1
1.0	3
1.5	8
1.8	15
1.9	18

The relationship between the k-value and porosity exhibits similarities to the findings reported by Zulkarnain et al. [66]. According to their results, there is a significant fall in thermal conductivity value when the pore volume fraction increases by up to 10%. The thermal conductivity exhibits a gradual reduction within the range of 10-20%. Once the value reaches 20%, it exhibits minimal reduction or remains rather steady.

Additionally, the third set of findings pertains to the fluctuation of the k-value based on the specific distribution type, as illustrated in Figure 6. The findings indicate that the k-value associated with the staggered distribution is lower compared to that of the in-line distribution, exhibiting a decrease of approximately 10-15%. The decrease in thermal conductivity can be due to the improved dispersion of air holes, which are distributed more evenly throughout the material. This distribution allows for more effective heat dissipation in a unidirectional manner, resulting in fewer thermal bridges. According to a study conducted by Fang et al. [57], it was observed through a simulation that the thermal conductivity of a nano-structured material with a zigzag arrangement exhibited lower values compared to other arrangements. This reduction in thermal conductivity was attributed to the impact of this particular distribution, which effectively hindered the movement of heat. Ordonez-Miranda and Alvarado-Gil [59] have demonstrated that an improved distribution of pores leads to a significant decrease in thermal conductivity, particularly when considering a high aspect ratio (the ratio between the longer and shorter dimensions of the pores). In addition, Skibinski et al. [68] have proposed the utilization of non-homogeneous distribution in the context of insulation materials.

The fourth set of findings pertains to the fluctuation of the k-value in relation to the shape of the pore. The findings, as depicted in Figure 7, indicate that the diamond form yields a lower k-value in comparison to other shapes, followed by the cubical shape, and lastly the sphere, which exhibits a higher heat transmission capability. The rationale for this phenomenon might be attributed to the enhanced heat reflection and resistance exhibited by multi-planar geometries compared to curved shapes [69]. The findings in the present study align with those reported by Wang et al. [70], who investigated the thermal conductivity of various pore shapes, including spheres, cubes, and T-shapes. The researchers have conducted an investigation on a silicone matrix material containing isolated pores that are filled with air. The findings of the study indicate that T-shaped pores had the lowest effective thermal conductivity, followed by cubical pores, while spherical pores demonstrated the highest effective thermal conductivity. The increased effective contact area of the T-shape was linked to this phenomenon, in comparison to other shapes. In a study conducted by Luo et al. [63], a comparison was made between the effective thermal conductivity of two geometric shapes, namely a cube and a triangle. The researchers observed that the thermal conductivity values of these geometries were found to be quite similar, with insignificant differences. Moreover, the assertion derived from the present findings may be incongruent with the one posited by Ordonez-Miranda and Alvarado-Gil [59]. In their study, the researchers have presented a thermal conductivity model based on a power law formulation. They have observed that the power exponent is at its lowest when considering spherical pores, while it increases for pores with non-spherical shapes. Nevertheless, it has been postulated that the aforementioned formula is more applicable to spherical and elliptical geometries as opposed to multi-planar configurations. Additionally, the formula fails to consider the anisotropy of the pore shape. Li et al. [67] have provided evidence that the k-value, which pertains to the geometry of the pore, is influenced by both the aspect ratio and the saturation degree. In addition, Babaei et al. [60] conducted a comparative analysis of the thermal conductivity across pores of varying shapes (cubic, triangular, and hexagonal) in terms of their anisotropy. The researchers also examined two distinct ways for calculation, namely parallel and perpendicular orientations. It has been discovered that the k-value exhibits its minimum value for a hexagonal form when the direction is perpendicular to its length, and its maximum value when the direction is parallel to it. Moreover, spherical pores show higher thermal disturbance propagation rate [71]. Also, the surface radiation greatly affects the heat transfer in the trapezoidal porous cavity [72].

In the current study, each figure in the results represents a certain category for one of the parameters under study, such as: quantity, size, shape and arrangement. However, it has been assumed that this procedure is effective, economic and easier to determine which case among all leads to the optimum k-values. As a result of the current analysis for the mentioned parameters, it can be noticed that in order to achieve a lower k-value (optimal value) under the given conditions, the specimen should possess 500 pore with pore diameter of 1.5 mm, characterized by a diamond shape and a staggered distribution. For this purpose, new specimens have been composed that have these characteristics, and tested for their k-values. The thermal conductivity values of these specimens yield 0.13 W/m·K for PLA and 0.12 W/m·K for ABS, as shown in Table 8. The observed values exhibit a decrease of around 40-45% in comparison to the

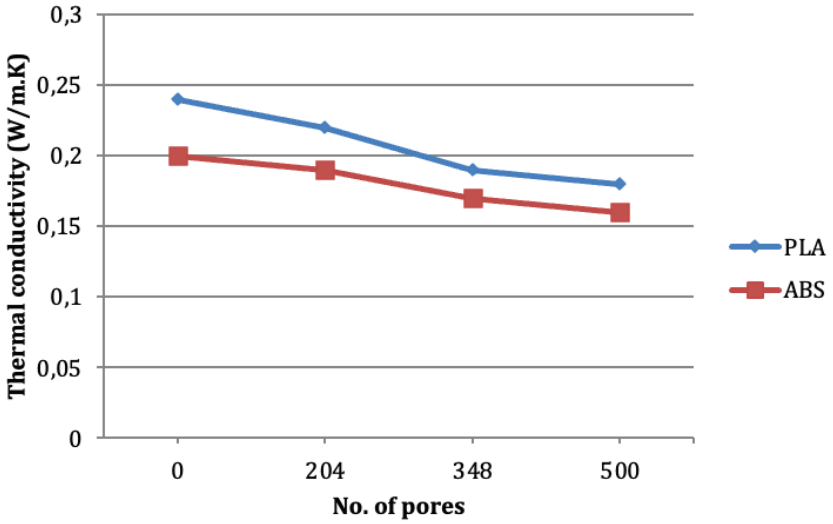

Figure 4. Results of thermal conductivity according to the number of pores (in-line 1 mm spherical pores).

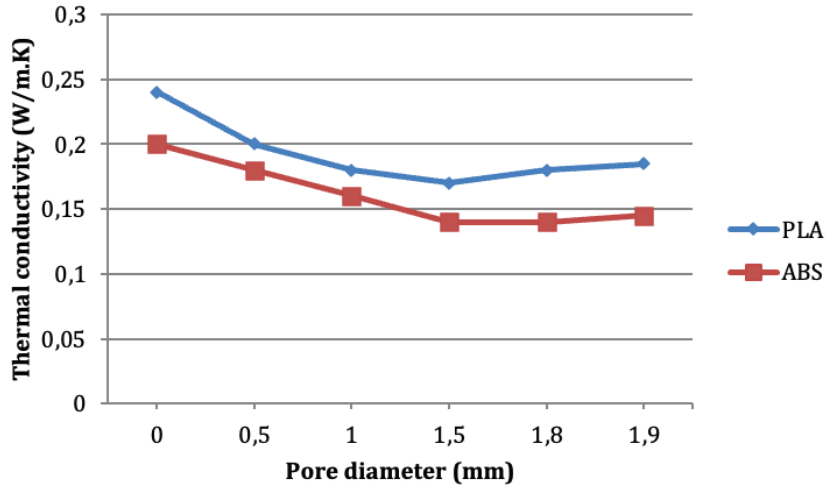

Figure 5. Results of thermal conductivity according to the pore diameter (500 in-line spherical pores).

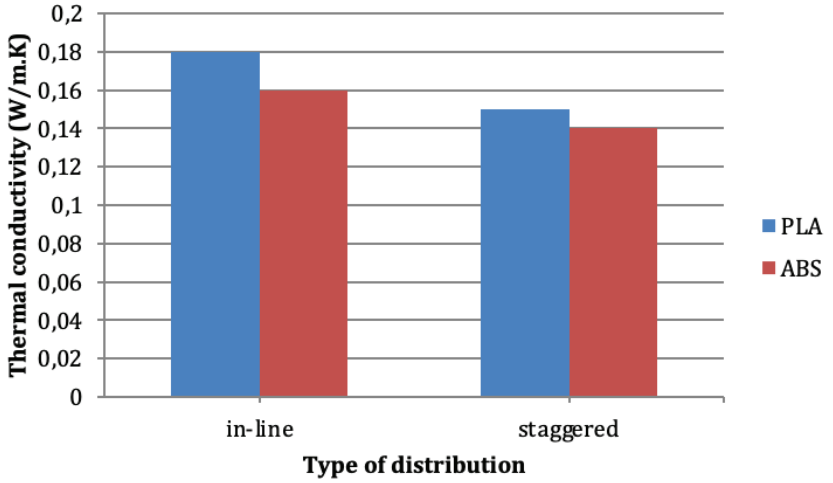

Figure 6. Results of thermal conductivity according to the type of distribution (500 spherical pores of 1 mm diameter).

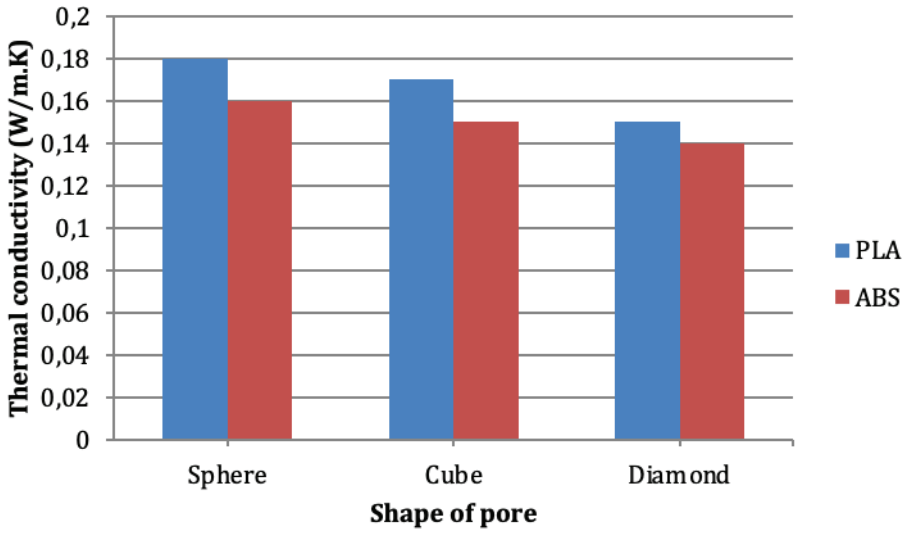

Figure 7. Results of thermal conductivity according to the shape of pore (500 in-line pores of 1 mm equivalent size).

non-porous samples of the same materials. Note that reference values are 0.24 W/m·K and 0.2 W/m·K for PLA and ABS, respectively.

Comparison with Previous Studies

In order to validate the findings of the present investigation, a comparison was made with the data obtained in prior studies, as presented in Table 9. The majority of the research included in this analysis focus on a limited range of design parameters, despite some variations in attributes or methodologies. The results of the study indicate that porous 3D printed samples exhibit greater efficiency compared to solid core samples, with a potential reduction in k-value of up to 75% in cryogenic temperature applications [31]. The use of hexagonal-shaped closers has been observed to yield certain enhancements [35]. Additionally, it has been shown that the sample exhibits a significant increase in strength, as well as enhanced thermal insulation capabilities, when a 30% in-fill density ratio is utilized [43, 73]. However, the majority of these investigations have indicated that there exists a restricted range of variance in the k-value (10-20%). This limited variation can be attributable to both the inaccuracies in the actual measurements and the precision of the theoretical assumptions. It should be noted that the data obtained in this study are applicable to specimens that are subjected to standard ambient conditions and possess adequate heat resistance. Nevertheless, the implementation of a reflecting layer has been proposed as a potential solution to reduce the elevated radiation rate [74]. Note that, the incorporation of nano-porous structures has a significant influence in reduce the k-value of polymer-based materials [46, 48]. Finally, when the air in the pores is replaced by vacuum, a notable decrease in the heat transfer can be achieved [75].

Table 8. Minimum k-values for different cases

It.	Case	Minimum k-value (W/m·K)	% Reduction in reference value
1	500 pores, spherical shape, diameter of 1 mm, in-line	0.16 for ABS	20
		0.18 for PLA	25
2	500 pores, spherical shape, diameter of 1.5 mm, in-line	0.14 for ABS	30
		0.17 for PLA	29
3	500 pores, spherical shape, diameter of 1 mm, staggered	0.14 for ABS	30
		0.15 for PLA	38
4	500 pores, diamond shape, diameter of 1 mm, in-line	0.14 for ABS	30
		0.15 for PLA	38
5	500 pores, diamond shape, diameter of 1.5 mm, staggered	0.12 for ABS	40
		0.13 for PLA	45

Table 9. Comparison with previous studies

Study	Materials and specifications	Results
Current	Materials: PLA and ABS (porous samples) No. of cavities: 200-500 Diameter of cavity: 0.5-1.9 mm Shape of cavity: sphere, cube and diamond Distribution: in-line and staggered Conditions: standard air conditions	Optimum k-value when the sample has 500 pores of 1.5 mm diameter, diamond shape and staggered distribution. The optimum k-value was 0.13 W/m·K for PLA and 0.12 W/m·K for ABS. These values are lower by 40-45% comparing to that of solid core samples.
[31]	Materials: PLA and ABS (solid samples) Conditions: very low temperatures	Optimum k-value was 0.05 W/m·K when the sample has very low temperature, where there is 75% reduction in k-value.
[35]	Materials: PA-12 (continuous closures used as hollowed window frame) No. of cavities: 100-1000 Diameter of cavity: 4-10 mm Shape of cavity: quadrangle, hexagonal, and triangle Distribution: fully Conditions: standard air conditions	Optimum k-value when the sample has 300 closers of 6 mm diameter, hexagonal shape and fully distributed. The optimum k-value was 0.06 W/m·K.
[38]	Materials: PLA (solid samples) of parallelepiped-shaped parts have 2-4 mm thicknesses. Conditions: standard air conditions	The main factors affect the thermal insulation capacity are the distance between the heat source and the test sample, as well as the thickness of the test sample.
[43]	Materials: PC (solid samples) Conditions: standard air conditions	Suitable insulation and strong sample has achieved a k-value of 0.065 W/m·K when the sample has 30% in-fill ratio, where there is 60% reduction in k-value.
[50]	Materials: PLA with porosity of 40-70%. Conditions: standard air conditions	There is a reduction in k-value down to 0.037 W/m·K. Energy saving by 45-65%.
[73]	Materials: EVA (hollow samples) with porosity of 50-70%. Conditions: standard air conditions	Suitable thermal insulation and fire-resistant material when the sample has 30% in-fill ratio.

CONCLUSION

The study investigates many effective parameters on the behavior of thermal conductivity of porous plastic material related to cavities, such as: number of cavities, shape, size and distribution. The utilized thermoplastics were poly-lactic acid (PLA) and acrylonitrile butadiene styrene (ABS), fabricated by 3D printing technology. The results gained from the study yielded the following observations:

1. The increasing of number of pores leads to decreasing of the k-value.
2. The k-value decreases by the increasing of the pore size until an optimum diameter. Beyond this diameter, the k-value turns up again.
3. The k-value for the staggered distribution is less than that of in-line distribution.
4. The sample of diamond pore shape has k-value comparing to other shapes, then cubical shape and lastly the sphere pore shape.
5. The analysis for minimum k-values revealed that optimum k-value, for the conditions applied in the current study, achieved when the 3D printed sample has 500 pores of 1.5 mm diameter, diamond shape and staggered distribution.
6. The lower thermal conductivity for optimum specimens results in a value of 0.13 W/m·K for PLA and 0.12 W/m·K for ABS. These values are lower by 40-45% comparing to that of solid core samples.

AUTHORSHIP CONTRIBUTIONS

Authors equally contributed to this work.

DATA AVAILABILITY STATEMENT

The authors confirm that the data that supports the findings of this study are available within the article. Raw data that support the finding of this study are available from the corresponding author, upon reasonable request.

CONFLICT OF INTEREST

The authors declared no potential conflicts of interest with respect to the research, authorship, and/or publication of this article.

ETHICS

There are no ethical issues with the publication of this manuscript.

REFERENCES

[1] Ebewele O. Polymer Science and Technology. 1st ed. Boca Raton: CRC Press; 2000. [CrossRef]

[2] Braun D, Cherdron H, Rehahn M, Ritter H, Voit B. Polymer Synthesis: Theory and Practice. 5th ed. New York: Springer; 2013. [CrossRef]

[3] Krevelen D, Nijenhuis K. Properties of Polymers. 4th ed. Amsterdam: Elsevier; 2009.

[4] Ehrenstein G. Polymeric Materials: Structure, Properties, Applications. 1st ed. Berlin: Hanser Verlag; 2001. [CrossRef]

[5] Tawfeeq M. Insulation Materials: Principles and Applications. 1st ed. Baghdad: Mustansiriyah University; 2021.

[6] Anh L, Pásztory Z. An overview of factors influencing thermal conductivity of building insulation materials. J Build Eng 2021;44:102604. [CrossRef]

[7] Li H, Zeng Q, Xu S. Effect of pore shape on the thermal conductivity of partially saturated cement-based porous composites. Cem Concr Compos 2017;81:87–96. [CrossRef]

[8] Shalwan A, Alajmi A, Yousif B. Theoretical study of the effect of fibre porosity on the heat conductivity of reinforced gypsum composite material. Polymers 2022;14:3973. [CrossRef]

[9] Liu H, Zhao X. Thermal conductivity analysis of high porosity structures with open and closed pores. Int J Heat Mass Transf 2022;183:122089. [CrossRef]

[10] Kosny J, Yarbrough D. Thermal Insulation and Radiation Control Technologies for Buildings. New York: Springer; 2022. [CrossRef]

[11] Hong S, Yu C, Hwang U, Kim C, Ri B. Effect of porosity and temperature on thermal conductivity of jennite: A molecular dynamics study. Mater Chem Phys 2020;250:123146. [CrossRef]

[12] Smith D, Alzina A, Bourret J, Nait-Ali B, Pennec F, Tessier-Doyen N, et al. Thermal conductivity of porous materials. J Mater Res 2013;28:2260–2272. [CrossRef]

[13] Sundarram S, Li W. On thermal conductivity of micro- and nanocellular polymer foams. Polym Eng Sci 2013;53:1901–1909. [CrossRef]

[14] Zhang H, Fang W, Li Z, Tao W. The influence of gaseous heat conduction to the effective thermal conductivity of nano-porous materials. Int Commun Heat Mass Transf 2015;68:158–161. [CrossRef]

[15] Yu H, Zhang H, Zhao J, Liu J, Xia X, Wu X. The thermal conductivity of micro/nano-porous polymers: Prediction models and applications. Front Phys 2022;17:23202. [CrossRef]

[16] Baetens R. High performance thermal insulation materials for buildings. In: Pacheco-Torgal F, Diamanti MV, Nazari A, Granqvist CG, Pruna A, Amirkhanian S. Nanotechnology in Eco-Efficient Construction. New Delhi: Woodhead Publishing; 2013. pp. 188–206. [CrossRef]

[17] Wang X, Niu X, Wang X, Qiu X, Istikomah N, Wang L. Thermal conductivity of porous polymer materials considering pore special-shape and anisotropy. eXPRESS Polym Lett 2021;15:319–328. [CrossRef]

[18] Presley M, Christensen F. Thermal conductivity measurements of particulate materials: 4. Effect of bulk density for granular particles. J Geophys Res 2010;115:E07003. [CrossRef]

[19] Østergaard M, Petersen R, König J, Bockowski M, Yue Y. Impact of gas composition on thermal conductivity of glass foams prepared via high-pressure sintering. J Non-Cryst Solids X 2019;1:100014. [CrossRef]

[20] Merillas B, Vareda J, León J, Rodríguez-Pérez M, Durães L. Thermal conductivity of nanoporous materials: where is the limit? Polymers 2022;14:2556. [CrossRef]

[21] Jasper L. Reconstructionism: IP and 3D Printing, SSRN, 2017. Available at: http://dx.doi.org/10.2139/ssrn.2842345. Accessed Jan 21, 2025. [CrossRef]

[22] Mirón V, Ferrándiz S, Juárez D, Mengual A. Manufacturing and characterization of 3D printer filament using tailoring materials. Procedia Manuf 2017;13:888-894. [CrossRef]

[23] MakerBot. 2020 Guide to 3D Printing Materials, 2020. Available at: https://cdn.cnetcontent.com/syndication/mediaserverredirect/e6b5204e10f48834b7bc52e4ebb89b69/original.pdf. Accessed Jan 21, 2025.

[24] 3D Learning Hub. Best Heat Resistant 3D Printing Materials, 2020. Available at: 25 May 2023. Available on: https://www.sculpteo.com/en/3d-learning-hub/3d-printing-materials-guide/heat-resistant-3d-printing/#:~:text=3D%20Printing%20material.-,Ultrasint%C2%AE%20PA6%20MF,and%20enhanced%20thermal%20distortion%20performance. Accessed Jan 21, 2025.

[25] He H, Zhan Z, Zhu Z, Xue B, Li J, Chen M, et al. Microscopic morphology, rheological behavior, and mechanical properties of polymers: Recycled acrylonitrile-butadienestyrene/polybutylene terephthalate blends. J Appl Polym Sci 2019;48310. [CrossRef]

[26] Jimenez-Perez J, Pincel P, Cruz-Orea A, Correa-Pacheco Z. Thermal characterization of a liquid resin for 3D printing using photothermal techniques. Appl Phys A 2016;122:556. [CrossRef]

[27] Billah K, Lorenzana F, Martinez N, Chacon S, Wicker R, Espalin D. Thermal analysis of thermoplastic materials filled with chopped fiber for large area 3D printing. Proceedings of the 30th Annual International Solid Freeform Fabrication Symposium–An Additive Manufacturing Conference, USA, August 12-14, 2019.

[28] Halim N, Mogan J, Sandanamsamy L, Harun W, Kadirgama K, Ramasamy D, et al. A review on 3D printed polymer-based composite for thermal applications. IOP Conf Ser Mater Sci Eng 2021;1078:012029. [CrossRef]
[29] Smith M, Kim S, Lambert A, Walde M, Lindahl J, Mungale K, et al. Maximizing the performance of a 3D printed heat sink by accounting for anisotropic thermal conductivity during filament deposition. 2019 18th IEEE Intersociety Conference on Thermal and Thermomechanical Phenomena in Electronic Systems (ITherm), Las Vegas, NV, USA, 2019. [CrossRef]
[30] formlabs. Guide to 3D Printing Materials: Types, Applications, and Properties, 2023. Available at: https://formlabs.com/asia/blog/3d-printing-materials/. Accessed May 22, 2023.
[31] Weiss K-P, Bagrets N, Lange C, Goldacker W, Wohlgemuth J. Thermal and mechanical properties of selected 3D printed thermoplastics in the cryogenic temperature regime. IOP Conf Ser Mater Sci Eng 2015;102:012022. [CrossRef]
[32] Wang B, Arias K, Zhang Z, Liu Y, Jiang Z, Sue H, et al. 3D printing of in-situ curing thermally insulated thermosets. Manuf Lett 2019;21:1–6. [CrossRef]
[33] Hu G, Cao Z, Hopkins M, Lyons J, Brennan-Fournet M, Devine D. Nanofillers can be used to enhance the thermal conductivity of commercially available SLA resins. Proc Manuf 2019;38:1236–1243. [CrossRef]
[34] Harris M. 3D Printing Materials for Large-Scale Insulation and Support Matrices [Doctoral dissertation]. Massey University; 2019.
[35] Grabowska B, Kasperski J. The thermal conductivity of 3D printed plastic insulation materials – The effect of optimizing the regular structure of closures. Materials 2020;13:4400. [CrossRef]
[36] Ibrahim Y, Elkholy A, Schofield J, Melenka G, Kempers R. Effective thermal conductivity of 3D-printed continuous fiber polymer composites. Adv Manuf Polym Compos Sci 2020;6:17–28. [CrossRef]
[37] Wang L, Feng J, Luo Y, Zhou Z, Jiang Y, Luo X, et al. Three-dimensional-printed silica aerogels for thermal insulation by directly writing temperature-induced solidifiable inks. ACS Appl Mater Interfaces. 2021;13(34):40964–40975. [CrossRef]
[38] Mihalache A, Hriţuc A, Boca M, Oroian B, Condrea I, Botezatu C, et al. Thermal insulation capacity of a 3D printed material. Macromol Symp 2021;396:2000286. [CrossRef]
[39] Zohdi N, Yang R. Material anisotropy in additively manufactured polymers and polymer composites: A review. Polymers 2021;13:3368. [CrossRef]
[40] Tirado-Garcia I, Garcia-Gonzalez D, Garzon-Hernandez S, Rusinek A, Robles G, Martinez-Tarifa J, et al. Conductive 3D printed PLA composites: On the interplay of mechanical, electrical and thermal behaviours. Compos Struct 2021;265:113744. [CrossRef]
[41] Ibrahim Y, Kempers R. Effective thermal conductivity of 3D-printed continuous wire polymer composites. Prog Addit Manuf 2022;7:699–712. [CrossRef]
[42] Panaite CE, Mihalache AM, Slătineanu L, Popescu A, Nagîţ G, Hriţuc A, et al. Numerical and experimental investigations of thermal conductivity of 3D printed polylactic acid. Macromol Symp 2022;404. [CrossRef]
[43] Bahar A, Belhabib S, Guessasma S, Benmahiddine F, Hamami A, Belarbi R. Mechanical and thermal properties of 3D printed polycarbonate. Energies 2022;15:3686. [CrossRef]
[44] Nemova D, Kotov E, Andreeva D, Khorobrov S, Olshevskiy V, Vasileva I, et al. Experimental study on the thermal performance of 3D-printed enclosing structures. Energies 2022;15:4230. [CrossRef]
[45] Cai Z, Thirunavukkarasu N, Diao X, Wang H, Wu L, Zhang C, et al. Progress of polymer-based thermally conductive materials by fused filament fabrication: A comprehensive review. Polymers 2022;14:4297. [CrossRef]
[46] An L, Guo Z, Li Z, Fu Y, Hu Y, Huang Y, et al. Tailoring thermal insulation architectures from additive manufacturing. Nat Commun 2022;13:4309. [CrossRef]
[47] Olcun S, Ibrahim Y, Isaacs C, Karam M, Elkholy A, Kempers R. Thermal conductivity of 3D-printed continuous pitch carbon fiber composites. Addit Manuf Lett 2023;4:100106. [CrossRef]
[48] Lee M, Sarkar A, Guo Z, Zhou C, Armstrong J, Ren S. Additive manufacturing of eco-friendly building insulation materials by recycling pulp and paper. Nanoscale Adv 2023;5:2547–2552. [CrossRef]
[49] Vahabi H, Laoutid F, Mehrpouya M, Saeb M, Dubois F. Flame retardant polymer materials: An update and the future for 3D printing developments. Mater Sci Eng R Rep 2023;144:100604. [CrossRef]
[50] Islam S, Bhat G, Sikdar P. Thermal and acoustic performance evaluation of 3D-printable PLA materials. J Build Eng 2023;67:105979. [CrossRef]
[51] Hosseinzadeh K, Mardani M, Paikar M, Hasibi A, Tavangar T, Nimafar M, et al. Investigation of second grade viscoelastic non-Newtonian nanofluid flow on the curve stretching surface in presence of MHD. Results Eng 2023;17:100838. [CrossRef]
[52] Rostami H, Najafabadi M, Hosseinzadeh K, Ganji D. Investigation of mixture-based dusty hybrid nanofluid flow in porous media affected by magnetic field using RBF method. Int J Ambient Energy 2022;43:6425–6435. [CrossRef]
[53] Mishra M, Panda J, Kumar D, Sahoo S. Thermal radiation and Soret effects on boundary layer flow past a vertical surface embedded in porous medium with induced magnetic field with reference to aluminum industry. J Therm Anal Calorim 2022;147:13829–13845. [CrossRef]
[54] Mavromatidis L, Bykalyuk A, El Mankibi M, Michel P, Santamouris M. Numerical estimation of

air gaps' influence on the insulating performance of multilayer thermal insulation. Build Environ 2012;49:227–237. [CrossRef]
[55] Schlanbusch R. A New Nano Insulation Material for Applications in Zero Emission Buildings [Master's thesis]. Norwegian University of Science and Technology; 2013.
[56] Braginsky L, Shklover V, Hofmann H, Bowen P. High-temperature thermal conductivity of porous Al2O3 nanostructures. Phys Rev B 2004;70:134201. [CrossRef]
[57] Fang T, Lee Z, Chang W, Huang C. Determining porosity effect on the thermal conductivity of single-layer graphene using a molecular dynamics simulation. Phys E Low Dimens Syst Nanostruct 2019;106:90–94. [CrossRef]
[58] Sumirat M, Yamamoto N, Shimamura S. Optimization of thermal and mechanical properties in nanoporous material. Transact Mater Res Soc Jpn 2011;36:281–284. [CrossRef]
[59] Ordonez-Miranda J, Alvarado-Gil J. Effect of the pore shape on the thermal conductivity of porous media. J Mater Sci 2012;47:6733–6740. [CrossRef]
[60] Babaei H, McGaughey A, Wilmer C. Effect of pore size and shape on the thermal conductivity of metal-organic frameworks. Chem Sci 2017;8:583–589. [CrossRef]
[61] Hu X, Gundlach B, Borstel I, Blum J, Shi X. Effect of radiative heat transfer in porous comet nuclei: case study of 67P/Churyumov-Gerasimenko. Astron Astrophys 2019;630:A5. [CrossRef]
[62] Kang S, Choi J, Choi S. Mechanism of heat transfer through porous media of inorganic intumescent coating in cone calorimeter testing. Polymers 2019;11:221. [CrossRef]
[63] Luo M, Wang C, Zhao J, Liu L. Characteristics of effective thermal conductivity of porous materials considering thermal radiation: A pore-level analysis. Int J Heat Mass Transf 2022;188:122597. [CrossRef]
[64] Yu H, Zhang H, Zhao J, Liu J, Xia X, Wu X. The thermal conductivity of micro/nano-porous polymers: Prediction models and applications. Front Phys 2022;17:23202. [CrossRef]
[65] Abuserwal A, Luna E, Goodall R, Woolley R. The effective thermal conductivity of open cell replicated aluminium metal sponges. Int J Heat Mass Transf 2017;108:1439–1448. [CrossRef]
[66] Zulkarnain M, Sharudin R, Ohshima M. Towards understanding of pore properties of polystyrene-b-polybutadiene-b-polystyrene (SEBS) foam effect on thermal conductivity using numerical analysis. Int J Technol 2022;13:533–543. [CrossRef]
[67] Li H, Zeng Q, Xu S. Effect of pore shape on the thermal conductivity of partially saturated cement-based porous composites. Cem Concr Compos 2017;81:87–96. [CrossRef]
[68] Skibinski J, Cwieka K, Haj Ibrahim S, Wejrzanowski T. Influence of pore size variation on thermal conductivity of open-porous foams. Materials 2019;12:2017. [CrossRef]
[69] Gündüz G. Thermodynamic characterization of planar shapes and curves, and the query of temperature in black holes. J Appl Math Phys 2021;9:2004-2037. [CrossRef]
[70] Wang X, Niu X, Wang X, Qiu X, Istikomah N, Wang L. Thermal conductivity of porous polymer materials considering pore special-shape and anisotropy. eXPRESS Polym Lett 2021;15:319–328. [CrossRef]
[71] Akbari S, Faghiri S, Poureslami P, Hosseinzadeh K, Mohammad Shafii B. Analytical solution of non-Fourier heat conduction in a 3-D hollow sphere under time-space varying boundary conditions. Heliyon 2022;8:e12496. [CrossRef]
[72] Alipour N, Jafari B, Hosseinzadeh K. Optimization of wavy trapezoidal porous cavity containing mixture hybrid nanofluid (water/ethylene glycol Go–Al2O3) by response surface method. Sci Rep 2023;13:1635. [CrossRef]
[73] Geoffroy L, Samyn F, Jimenez M, Bourbigot S. Innovative 3D printed design to conceive highly fire-retardant multi-material. Polym Degrad Stab 2019;169:108992. [CrossRef]
[74] Abdulsada G, Salih T. Experimental and theoretical study for the performance of new local thermal insulation in Iraqi building. In: Sayigh A, ed. Renewable Energy in the Service of Mankind. Vol I. New York: Springer; 2015. [CrossRef]
[75] Ray S, Tripathy A, Sahoo S, Bindra H. Performance analysis of receiver of parabolic trough solar collector: Effect of selective coating, vacuum, and semitransparent glass cover. Int J Energy Res 2018;42(13):4235–4249. [CrossRef]